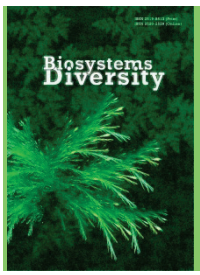

Biosystems Diversity

ISSN 2519-8513 (Print)
ISSN 2520-2529 (Online)
Biosyst. Divers.,
2024, 32(3), 389–397
doi: 10.15421/012442

Assessing landslide susceptibility in Chefchaouen, Morocco: An application of the landslide numerical risk factor method for sustainable urban development and disaster risk management

L. Dahmani*, S. Laaribya*, H. Naim*, V. Tunguz**, T. Dindaroglu***

*Ibn Tofail University, Kenitra, Morocco
**University of East Sarajevo, East Sarajevo, Bosnia and Herzegovina
***Karadeniz Technical University, Trabzon, Turkey

Article info

Received 28.06.2024
Received in revised form 05.08.2024
Accepted 21.08.2024

Ibn Tofail University, B.P. 242, Kenitra, Morocco. Tel.: +212-661-403-557. E-mail: lahcen.dahmani@uit.ac.ma

University of East Sarajevo, East Sarajevo, Republic of Srpska, Bosnia and Herzegovina. Tel.: +387-57-340-401. E-mail: office@pof.ues.rs.ba

Karadeniz Technical University, Trabzon, Turkey. Tel.: +90-462-377-2801. E-mail: orman@ktu.edu.tr

Dahmani, L., Laaribya, S., Naim, H., Tunguz, V., & Dindaroglu, T. (2024). Assessing landslide susceptibility in Chefchaouen, Morocco: An application of the landslide numerical risk factor method for sustainable urban development and disaster risk management. Biosystems Diversity, 32(3), 389–397. doi:10.15421/012442

This research investigates landslide susceptibility in Chefchaouen, Morocco, using the Landslide Numerical Risk Factor (LNRF) method to inform sustainable urban development and disaster risk management. The study incorporates local factors such as geological characteristics, climatic conditions, land use patterns, and gravitational influences within the LNRF framework. The results demonstrate that slope, altitude, geological complexity, and precipitation are key determinants of landslide susceptibility, with complex geology and high rainfall significantly increasing risk. The research highlights the critical need for forest conservation, reforestation, and responsible land management to mitigate the heightened landslide vulnerability caused by human activities such as deforestation, overexploitation, and urban expansion. The study provides valuable insights for enhancing regional planning and natural resource management to reduce landslide risks effectively.

Keywords: landslide susceptibility; geological risk assessment; urban planning; natural disaster management; environmental sustainability.

Introduction

Assessing landslide susceptibility in each region is essential for natural hazard management and urban planning (Lissak et al., 2020; Yong et al., 2022; Alcántara-Ayala & Sassa, 2023). The Numerical Landslide Risk Factor (LNRF) represents an innovative approach that integrates geographical data and influencing factors to generate landslide susceptibility maps (Arabameri et al., 2019; Sur et al., 2021). This method classifies areas according to their likelihood of landslides, providing a valuable tool for identifying the most sensitive areas and taking preventive measures (Patil et al., 2020; Yong et al., 2022). Influencing factors incorporated into the LNRF method include geology, geomorphology, slope, elevation, lineaments, specific erosion potential index (SPI), precipitation, soil type, land use, and other topographical and climatic parameters (Abedini & Tulabi, 2018) The combination of remote sensing and geographic information system (GIS) data improves the accuracy of landslide susceptibility mapping, offering a valuable resource for decision-makers and engineers in implementing preventive measures (Taalab et al., 2018; Roy & Saha, 2019).

Land Use and Land Cover (LULC) changes significantly affect landslide susceptibility (Pacheco Quevedo et al., 2023). In Chefchaouen, slope instability cases are related to the subsoil layers and affect the stability of newly built districts (El Kharim et al., 2021). Rapid urban growth and LULC changes can increase landslide risks. Future LULC scenarios reveal a potential increase in landslide susceptibility (Tyagi et al., 2023). Therefore, proper land use policies are crucial for sustainable development.

The province of Chefchaouen in Morocco's north-western Rif includes dense forest areas, matorrals or scrubland, agricultural land, bare land, urbanized areas, and bodies of water. Chefchaouen, a picturesque town in Morocco's north-western Rif region, provides a relevant example for the application of LNRF. The mountainous region in which Chefchaouen nestles features rugged relief, limestone, sandstone and marl formations, as well as rivers running through the town (Laaribya et al., 2024). Climatic conditions with high winter precipitation, influenced by the North Atlantic Oscillation (NAO), accentuate the risks of gravitational movements such as landslides and gullying (El Kharim et al., 2021; Dahmani et al., 2024). The Chefchaouen region is prone to landslides, debris flows and collapses caused by gravitational displacements, which are governed by geology, topography, and land use (Obda et al., 2024).

Chefchaouen, as a tourist destination prized for its distinctive architecture and mountainous landscapes, must take natural hazards into account in its tourism planning and urban development. This study aims to apply the LNRF method to Chefchaouen, integrating local factors of geology, climate, land use and gravity movements to assess landslide susceptibility. The results of this research will provide crucial information for natural hazard management and urban planning in the Chefchaouen region, and serve as a model for other regions facing similar challenges.

Materials and methods

Study area. Chefchaouen, located in northern Morocco, enjoys a warm and temperate climate. The average annual temperature is 15.3 °C. The region receives about 878 mm of precipitation each year. July is the driest month with only 3 mm of rainfall, while November is the wettest month with an average of 117 mm of rainfall. August is the hottest month of the year with an average temperature of 24.4 °C. In contrast, January is the coldest month with an average temperature of 8.2 °C (Obda et al., 2024). As part of the Rifaine chain (Northern Morocco), Chefchaouen province boasts highly complex geological and morphological features (Fig. 1). Chefchaouen lies at a major structural junction, where the massive Triassic and Jurassic carbonate rocks of the Dorsale Calcaire structural unit are superimposed on the more recent Cretaceous clay formations of the Tangier parautochthonous unit.

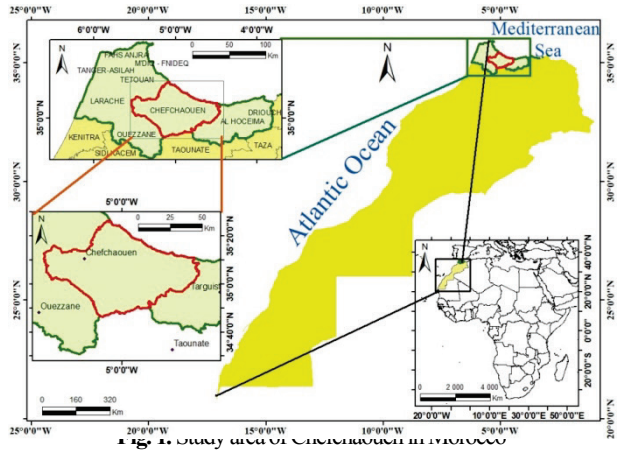

Fig. 1. Study area of Chefchaouen in Morocco

This geological transition zone is marked by a low-angle thrust fault, revealing the displacement of tectonic thrust sheets to the southwest of the range. In addition, a third tectonic unit, called "Predorsal", consisting of sandstone and clay, is present in areas devoid of boulder deposits (Gwinn, 1987; Ouahabi et al., 2018). The relief of Chefchaouen illustrates the contrast between these different tectonic units. The landscape evolves from steep rocky reliefs at higher altitudes to gentler clay slopes downstream. This topographical pattern is the result of differentiated erosion processes and the slow movement of clay formations, giving rise to a rugged topography with poor drainage. The terrain features flat, counter-sloping surfaces, with some areas showing deposits of ancient carbonate slopes tinted red to buff (El Kharim et al., 2021).

Taken as a whole, Chefchaouen's geological and morphological features play a decisive role in shaping the landscape, influencing the city's urban development and its vulnerability to natural hazards such as landslides (Papathoma-Köhle et al., 2007; Rovero & Fratini, 2013; El Kharim et al., 2021).

Methodology of LNRF. The study of landslide susceptibility in the province of Chefchaouen (Northern Morocco) involved several stages. Firstly, past landslide events were identified. Next, the influencing factors needed to model landslide susceptibility were prepared (Fig. 2). These factors were mapped to understand their influence on landslides. Using these data, an LNRF model was established to map landslide susceptibility in the region. Finally, the accuracy of this susceptibility mapping was assessed to validate the results obtained.

In our study, we adapted the recent landslide inventory from the period 2014 to 2019 with influencing factors such as geology, slope, elevation, precipitation, soil, land use, etc. The GEOBIA method was employed to extract landslides and generate a landslide inventory map for the study region. This approach identified the most landslide-prone areas and provided valuable information for risk management.

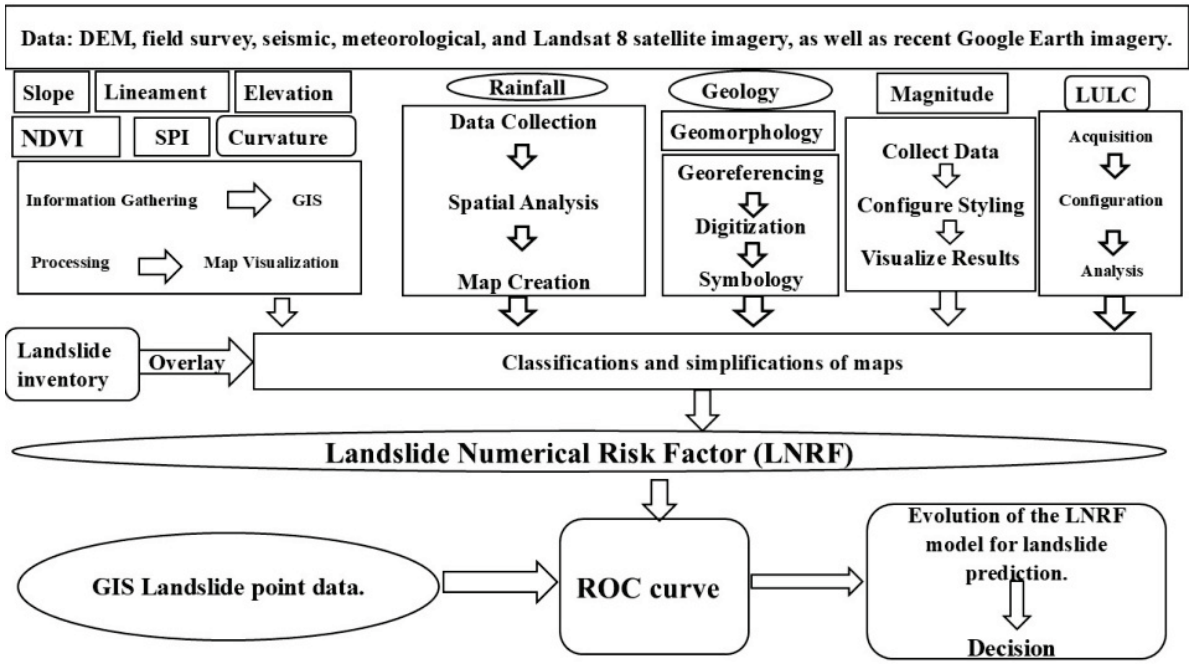

Fig. 2. Flow chart of work methodology

Table 1
Spectral and topographic indices developed and reference

Acronym	Spectral and topographic index	Formula	References
NDVI	Normalized difference vegetation index	(NIR-RED)/(NIR+RED)	Lahcen et al. (2022)
Curvature	Standard curvature	(profile curvature (PrCurv)) + (planform curvature (PlCurv))/2	Patil & Panhalkar (2023)
Slope	Slope	derived from a Digital Elevation Model (DEM)	Marín-Rodríguez et al. (2024), El Kharim et al. (2021)
Geology	Geology	Geological study based on field data and maps	El Kharim et al. (2021)
Magnitude	Magnitude	Seismic magnitude study based on field data	Obda et al. (2024)
Soil type	Soil type	Soil Typology, Data, and Prior Studies	El Kharim et al. (2021)
Rainfall	Rainfall	Rainfall from meteorological data	El Kharim et al. (2021), Yang et al. (2023)
Geomorphology	Geomorphology	Geomorphology based on field data and previous studies	Obda et al. (2024)
SPI	Standardized precipitation index	$= \Phi^{-1} P$	Şen & Şişman (2024)
Lineament	Lineament	Lineament, based on field data	Sadiq et al. (2022)
Elevation	Elevation	derived from a Digital Elevation Model (DEM)	Ibrahim et al. (2020)
LULC	LULC (land use/land cover)	based on very recent Landsat 8 satellite imagery and Google Earth	Pande et al. (2024)
LNRF	Numerical landslide risk factor	$LNRF = \frac{A}{E}$	Abedini & Tulabi (2018)

– SPI: This can stand for various things depending on the context, but in finance, for example, it often stands for Standardized Precipitation Index1.

– Φ^{-1}: This is commonly used to denote the inverse of a function or matrix, referred to as Phi inverse or inverse of Φ.

– P: The letter P can represent a variety of concepts depending on the context. For instance, in mathematics, it could represent a point, probability, or power.

This is commonly used to denote the inverse of a function or matrix, referred to as Phi inverse or inverse of Numerical Landslide Risk Factor (LNRF).

The Numerical Landslide Risk Factor (LNRF) is a method used to assess landslide susceptibility in hilly regions. It integrates several influencing factors such as geology, geomorphology, slope, elevation, precipitation, soil, etc., to determine areas at high risk of landslides. LNRF values above 1 indicate a high responsibility of the influencing factors in landslide occurrences, while values below 1 suggest a lesser influence(Abedini & Tulabi, 2018; Wang et al., 2021; Method & Bahnassy, 2023).

Results

Slope. Slope of the study area (Chefchaouen) is distributed as follows: between 0 and 14 degrees covers 37.8% of the surface, between 15 and 34 degrees represents 55.9% of the surface, between 35 and 54 degrees occupies 6.2% of the surface, and between 55 and 75 degrees covers only 0.08% of the surface (Fig. 3).

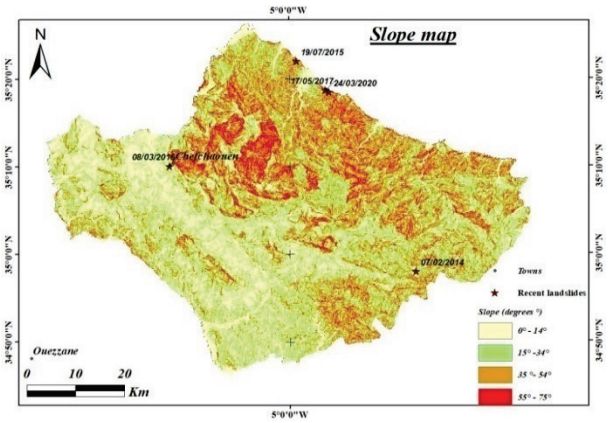

Fig. 3. Slope map of the study area

Altitude. 7% of the surface of Chefchaouen province lies between 0 and 238 meters altitude, 15% between 238 and 418 meters, 17% between 418 and 580 meters, 15% between 580 and 746 meters, 13% between 746 and 921 meters, 11% between 921 and 1108 meters, 10% between 1108 and 1308 meters, 7% between 1308 and 1541 meters, and 4% between 1541 and 2149 meters (Fig. 4).

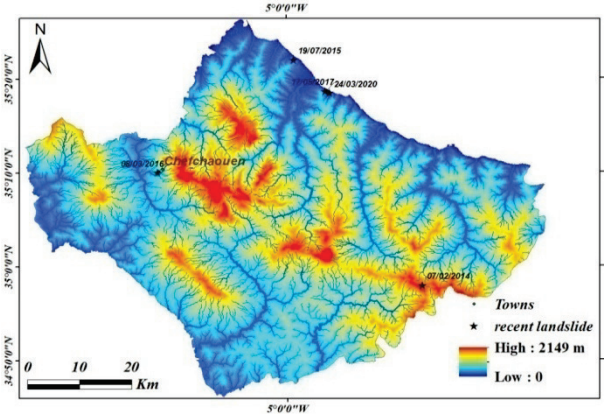

Fig. 4. Altitude of Chefchaouen study area in meters

Geology. The geology of Chefchaouen province shows a diversity of rock formations. Shales, sandstones and conglomerates account for a significant share of the territory, with 21.6% and 2.1% of the surface, while other similar formations have smaller percentages, at 1.84%, 0.31%, 0.25% and 4.24%. Dolomites, marls and limestones are also present, covering 17.08%, 0.16%, 11.33% and 1.78% of the surface. Archean Precambrian rocks, notably gneisses and micaschists, occupy 7.08% and 1.14% of the surface. Schists and micaschists are also present at 4.24%, 0.35% and 0.22%. Peridotite is present at 1.80% of the surface. Finally, the synclinal basin occupies a significant 21.59% of the province's total surface area (Fig. 5).

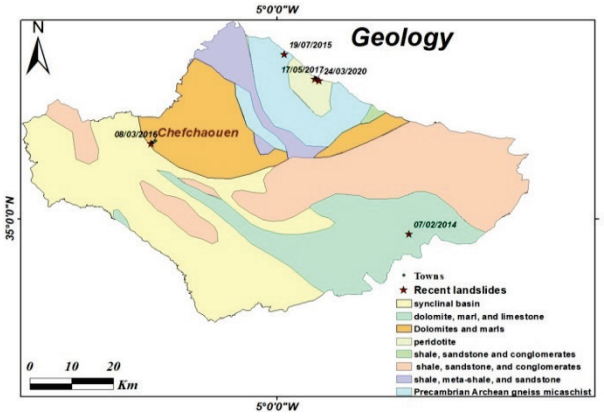

Fig. 5. Geological map (after El Kharim et al., 2021, modified and simplified)

Lineament. The map of Chefchaouen reveals distinct lineaments, commonly known as alignments, visible across its landscape. These alignments are characterized by specific distances and cover varied areas. For example, alignments spaced 400 meters apart cover an area of 2,255 km^2. As the distance increases to 800 meters, the area decreases to 1,367 km^2. Alignments spaced at 1,200 meters cover 488 km^2, those at 1,600 meters cover 155 km^2, and alignments spaced at 2,000 meters cover 133 km^2 (Fig. 6).

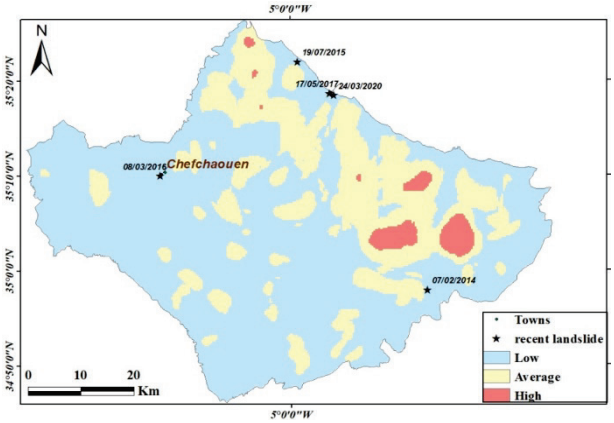

Fig. 6. The line distance map

Precipitation. Chefchaouen, located in the north of Morocco, experiences high precipitation due to orographic rainfall. Weather stations in the region record an average annual precipitation ranging from 899 to 1154 mm (Fig. 7). This precipitation is primarily observed during January and February.

Land use and land cover (LULC). The province of Chefchaouen is comprised of built-up areas, which occupy 12% of its surface. Dense forests cover 19% of the region, while plantations occupy 14%. Agricultural areas cover 21% of the province. Mixed zones, combining residential and agricultural uses, account for 11% of the area. Other unspecified land uses occupy 17% of the province. Water bodies cover 7% of the total surface area (Fig. 8).

Normalized Difference Vegetation Index (NDVI). Areas with an NDVI between –0.08 and 0.12 cover 15% of the province's surface. Areas with an NDVI between 0.12 and 0.16 represent 32% of the surface. Areas with an NDVI between 0.16 and 0.21 cover 27% of the surface. Areas with an NDVI between 0.21 and 0.27 cover 18% of the surface. Areas with an NDVI between 0.27 and 0.50 cover 8% of the surface (Fig. 9).

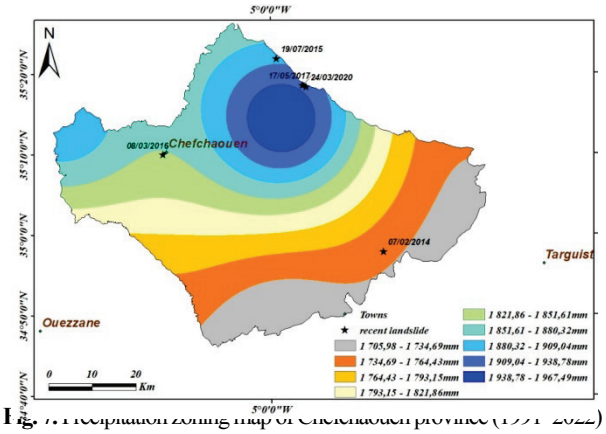

Fig. 7. Precipitation zoning map of Chefchaouen province (1991-2022)

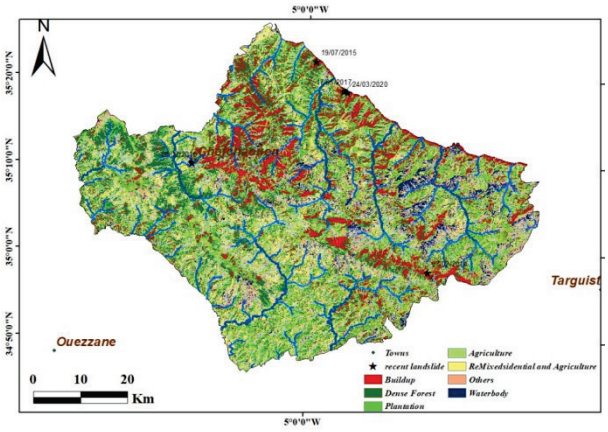

Fig. 8. LULC map of the study area

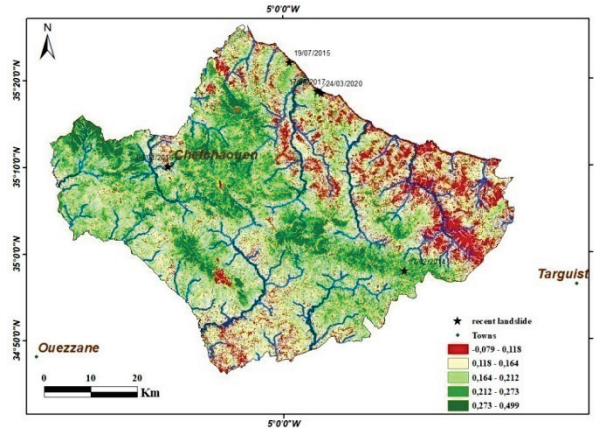

Fig. 9. NDVI map of study area – Chefchaouen

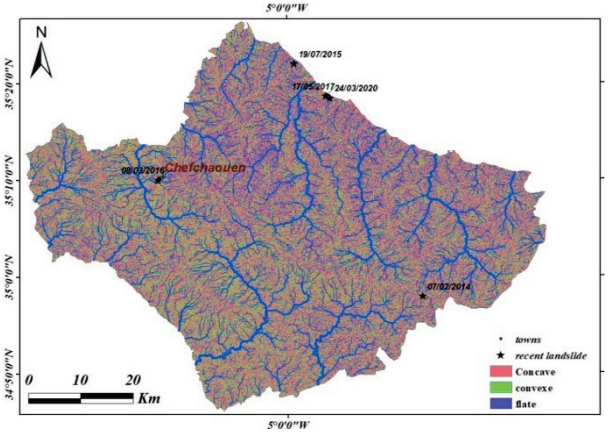

Fig. 10. Topographic curvature map

Distribution of topographic curvature (Curvative). Concave areas account for 55% of the province's surface. Convex areas occupy 28% of the surface. Flat areas cover 17% of the surface (Fig. 10).

Geomorphology. The province of Chefchaouen, located in the Cordillera del Rif, is predominantly mountainous with a varied geomorphology. The concave zones, representing 55% of the surface, are associated with the terrains of the Inner Domain, mainly Paleozoic and metamorphic. Convex zones, covering 28%, correspond to the limestone Dorsale of the Inner Domain. The flat areas, covering 17% of the surface, are linked to the Flysch or the Outer Domain. The relief is accentuated by Jbel Lakraa, culminating at 2159 meters (Fig. 11).

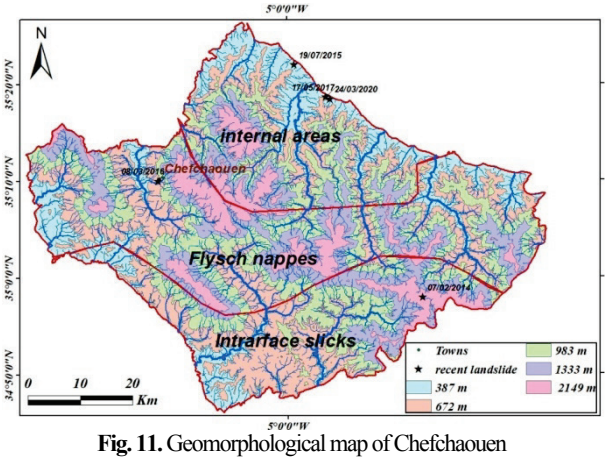

Fig. 11. Geomorphological map of Chefchaouen

Flux power index (SPI). For Chefchaouen province, the SPI is used to assess drought or moisture conditions in the region. The average annual rainfall is relatively high, but its distribution varies from year to year (Fig. 12).

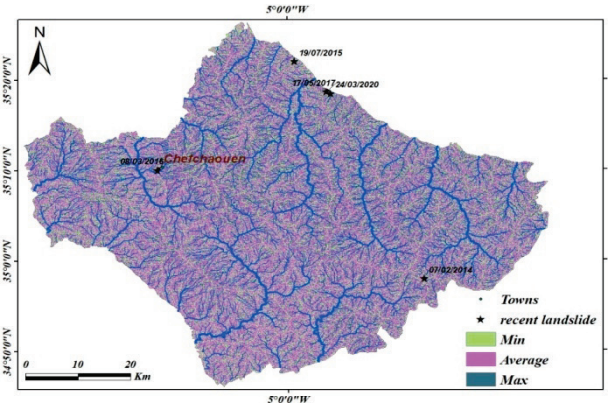

Fig. 12. SPI

In terms of NDVI, the zone with an NDVI between 0.08 and 0.12 covers 15% of the total area and 70% of the landslide area. The NDVI zones from 0.12 to 0.16 and from 0.16 to 0.21 cover 32% and 27% of the total area, respectively, with no landslide area. The NDVI zone from 0.21 to 0.27 covers 18% of the total area and 30% of the landslide area. The NDVI zone from 0.27 to 0.50 covers 8% of the total area with no landslide area (Fig. 13, Table 2).

In terms of curvature, the concave zone represents 55% of the total area and 16% of the landslide area. The convex zone accounts for 28% of the total area and 54% of the landslide area. The flat zone covers 17% of the total area and 30% of the landslide area (Fig. 13, Table 2).

Regarding lineaments, the 400-meter lineament zone covers 51% of the total area and 44% of the landslide area. The 800-meter lineament zone accounts for 31% of the total area and 30% of the landslide area. The 1200-meter lineament zone represents 11% of the total area and 26% of the landslide area. The 1600-meter and 2000-meter lineament zones cover 4% and 3% of the total area, respectively, with no landslide area (Fig. 13, Table 2).

Magnitude zones in Chefchaouen province include:

–Zones with magnitude from 0.00 to 0.93 cover 0.39% of the surface;

– Zones from 1.40 to 2.33 cover 0.47% and 0.74% of the surface, respectively;
– Zones from 2.33 to 2.80 cover 1.74% of the surface.
– Zones from 2.80 to 3.27 cover 4.49% of the surface.
– Zones from 3.27 to 3.73 cover 87.62% of the surface;
– Zones from 3.73 to 4.19 cover 3.30% of the surface (Fig. 13, Table 2).

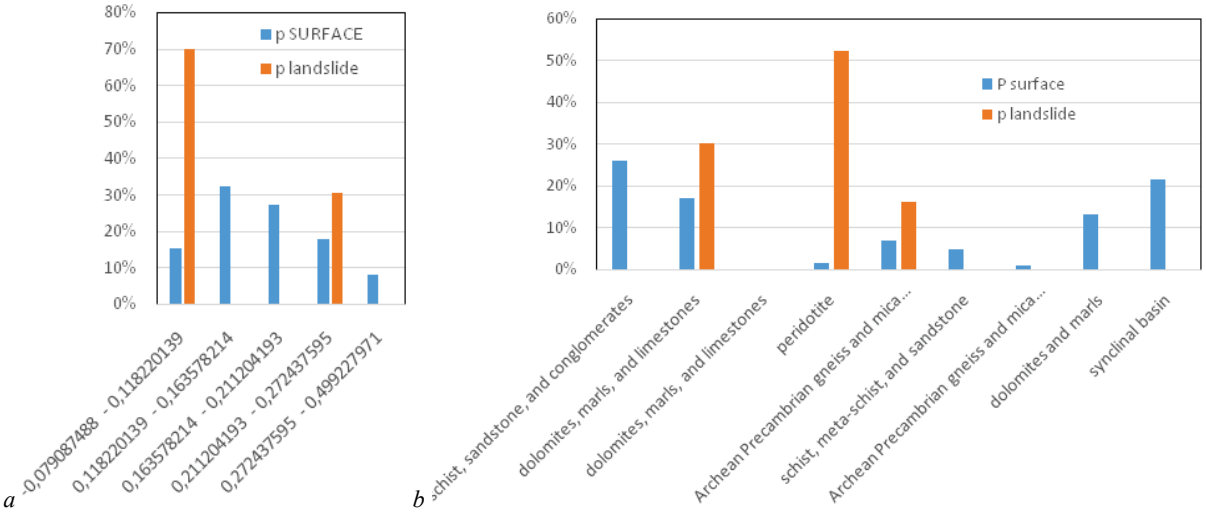

Fig. 13. Factor graphs showing the percentage of landslides as a function of the percentage of the surface area of the factors used to influence landslide: *a* – NDVI, *b* – geology

Table 2
Integrated landslide risk analysis: Combining influencing factors with the LNRF Layer

	Class interval		Methods	Area, %	Landslides area, %	LNRF	Fuzzy membership values using LNRF model	Weight	Instability
Rainfall, mm	1 706	1 735	natural pause	14	0	0	0	0	low
	1 735	1 764		16	30	2.72	0.58	2	average
	1 764	1 793		11	0	0	0	0	low
	1 793	1 822		11	0	0	0	0	low
	1 822	1 852		12	1	0.13	0.03	0	low
	1 852	1 880		14	0	0	0	0	low
	1 880	1 909		10	16	1.45	0.31	2	average
	1 909	1 939		6	52	4.7	1	2	average
	1 939	1 967		5	0	0	0	0	low
Slope	0	14	natural pause	37.8	28	1.12	0.84	1	high
	15	34		55.9	30	1.21	1	1	high
	35	54		6.2	26	1.03	0.68	1	high
	55	75		0.1	16	0.64	0	0	low
Altitude, m	0	238	natural pause	7	68	6.15	1	2	average
	238	418		15	0	0	0	0	low
	418	580		17	1	0.13	0.02	0	low
	580	746		15	0	0	0	0	low
	746	921		13	0	0	0	0	low
	921	1108		11	0	0	0	0	low
	1108	1308		10	0	0	0	0	low
	1308	1541		7	0	0	0	0	low
	1541	2149		4	30	2.72	0.44	2	average
Geology	shale. sandstone. and conglomerates			22	0	0	0	0	low
	dolomite. marl and limestone			17	30	4.54	0.58	2	average
	shale. sandstone and conglomerates			2	0	0	0	0	low
	dolomite. marl and limestone			0	0	0	0	0	low
	shale. sandstone and conglomerates			2	0	0	0	0	low
Geology	shale. sandstone and conglomerates			0	0	0	0	0	low
	peridotite			2	52	7.84	1	2	average
	Precambrian Archean gneiss micaschist			7	16	2.41	0.31	2	average
	shale. sandstone and conglomerates			0	0	0	0	0	low
	schist, meta-schist, and sandstone			4	0	0	0	0	low
	schist, meta-schist, and sandstone			0	0	0	0	0	low
	schist, meta-schist, and sandstone.			0	0	0	0	0	low
	Precambrian Archean gneiss micaschist			1	0	0	0	0	low
	dolomite and marl			11	1	0.21	0.03	0	low
	dolomite and marl			2	0	0	0	0	low
	cuvute synclinal			22	0	0	0	0	low
LULC	Built up			12	30	2.12	0.44	2	average
	Dense Forest			19	0	0	0	0	low
	Plantation			14	68	4.79	1	2	average
	Agriculture			21	0	0	0	0	low

	Class interval		Methods	Area, %	Landslides area, %	LNRF	Fuzzy membership values using LNRF model	Weight	Instability
	Mixed			11	0	0	0	0	low
	Others			17	0	0	0	0	low
	Waterbody			7	1	0.1	0.02	0	low
Magnitude	0.001	0.468		0.4	0	0	0	0	low
	0.468	0.934		0.4	0	0	0	0	low
	0.934	1.401		0.5	0	0	0	0	low
	1.401	1.867		0.7	0	0	0	0	low
	1.867	2.334		1.7	0	0	0	0	low
	2.334	2.800		4.5	0	0	0	0	low
	2.800	3.267		87.6	100	9	1	2	average
	3.266	3.733		3.3	0	0	0	0	low
	3.733	4.199		0.9	0	0	0	0	low
SPI	Min			28	0.9	0	0	0	low
	Average			47	73	2.2	1.1	2	average
	max			24	27	0.8	0.4	1	high
Structural	zones internes			26	68	2.05	1	2	average
	Flysch nappes			47	1	0.04	0	0	low
	intrarifain nappes			27	30	0.91	0.43	1	high
Curvature	concave			55	16	0.48	0	0	low
	convex			28	54	1.61	1	2	average
	flat			17	30	0.91	0.38	1	high
Lineament	400			51	44	2.2	1	2	average
	800			31	30	1.51	0.69	2	average
	1200			11	26	1.28	0.58	1	high
	1600			4	0	0	0	0	low
	2000			3	0	0	0	0	low
NDVI	0.0798	0.1189		15	70	3.49	1	2	average
	0.118	0.1634		32	0	0	0	0	low
	0.163	0.2113		27	0	0	0	0	low
	0.211	0.2725		18	30	1.51	0.43	2	average
	0.272	0.499		8	0	0	0	0	low

Landslide susceptibility map. The stability assessment of the region reveals that most class intervals are characterized by low instability, indicating relative stability. However, one specific interval class, ranging from 3 to 4, shows moderate instability. This class represents 88% of the total area and encompasses 100% of the landslide area, suggesting that this region is potentially unstable and could be prone to future landslides. Other parameters such as LNRF, fuzzy membership values, weight, and magnitude are all zero for all interval classes. This may indicate that these parameters were not included in the analysis or have no significant impact on the region's instability. It is noteworthy that magnitude is a crucial parameter in many geological models, and its zero value might warrant further investigation.

From the table data:

– the Min class interval, representing 28% of the total area and 0.90% of the landslide area, shows low instability, indicating relative stability;

– the Medium class interval, covering 47% of the total area and 73% of the landslide area, exhibits medium instability. This region has a weight of 2.2 and a magnitude of 1.1, suggesting moderate instability;

– the Max class interval, accounting for 24% of the total area and 27% of the landslide area, shows high instability, with a weight of 0.8 and a magnitude of 0.4, indicating significant instability.

Regarding geomorphology:

– the Inner Zone, which covers 26% of the total area and 68% of the landslide area, is moderately unstable. With a weight of 2.05 and a magnitude of 1, this zone indicates moderate instability;

– the Flysch Nappes Zone, representing 47% of the total area and only 1% of the landslide area, exhibits low instability with a weight of 0.04, indicating relative stability;

– the Nappes intra rifaines Zone, covering 27% of the total area and 30% of the landslide area, is highly unstable with a weight of 0.91 and a magnitude of 0.43, reflecting high instability (Fig. 14 and 15).

Discussion

Slope is a crucial topographical factor in the study of landslides. A steep slope is often associated with an increased risk of landslides, as it favors the downward movement of rocks and debris under the influence of gravity. Slope analysis helps to identify areas at high risk of landslides, and to take preventive measures to reduce the impact of natural disasters (Gruzelle & Lebaut, 2022). Steeper slopes are generally more susceptible to landslides, as the force of gravity acts more directly to move the soil downhill. In our study, the slope varied between 0 and 74°. Note that instability is strong for slopes between 0 and 54 degrees, LNRF = 1, Fuzzy membership values using LNRF model between 0.68 and 1, suggesting that these slopes are steep enough to promote instability (Table 2). Altitude is another important factor in the study of landslides. Research shows that landslides are more likely to occur at higher altitudes, particularly in mountainous regions. Variations in altitude can influence precipitation distribution, soil saturation and slope stability, all key elements in landslide susceptibility (Nakileza & Nedala, 2020). Altitude can influence terrain instability in several ways. For example, higher altitudes may be associated with more extreme weather conditions, which can increase instability. In addition, soils at higher altitudes may be less well developed and therefore more susceptible to movement. In our case, altitude varies between 0 and 2149 m. Note that instability is average at low altitudes in regions close to the sea (0 to 238 m), where we find a value of 6.15 for LNRF, the landslide area reaches 68% and concerns high altitudes (1541 to 2149 m). LNRF = 2.72, landslide area is 30%, instability is also high (Table 2).

Chefchaouen's geology features a complex juxtaposition of geological units, with the massive Triassic and Jurassic carbonate rocks of the Dorsal limestone unit underlying the Cretaceous clay formations of the Tangier unit. This geological configuration is marked by a low angle thrust fault, indicating major tectonic movements. The presence of a third tectonic unit, the Predorsalian, adds to the geological complexity of the region (Mastere et al., 2013). Chefchaouen's relief morphology is the result of these geological features, with steep rocky reliefs contrasting with gentle clay slopes. These features have been shaped by processes of differential erosion and slow movement of the clay formations, creating a rugged topography with poor drainage. In addition, the region has a high relative humidity due to orographic precipitation (Margreth, 2017; Doljin & Yembuu, 2021; El Kharim et al., 2021). Chefchaouen's geology plays an essential role in shaping the landscape and directly influences slope stability, vulnerability to landslides and the region's urban development (Bouchra et al., 2020). The type of soil or rock can greatly affect ground

instability. Certain types of soil, such as clays, are more susceptible to landslides because they tend to retain water and become very slippery when wet. In Table 2, certain soil types such as dolomites, marls and limestones show a LNRF value = 4.54, Fuzzy membership values using LNRF model 0.52 and average instability, landslide percentage 30. Peridotite landslide surface 52, LNRF = 7.52, Fuzzy membership values using LNRF model = 1 strong instability and Precambrian Archean gneiss micaschist show medium instability LNRF = 2.41, Fuzzy membership values using LNRF model = 2, which may indicate that they have properties that favor instability.

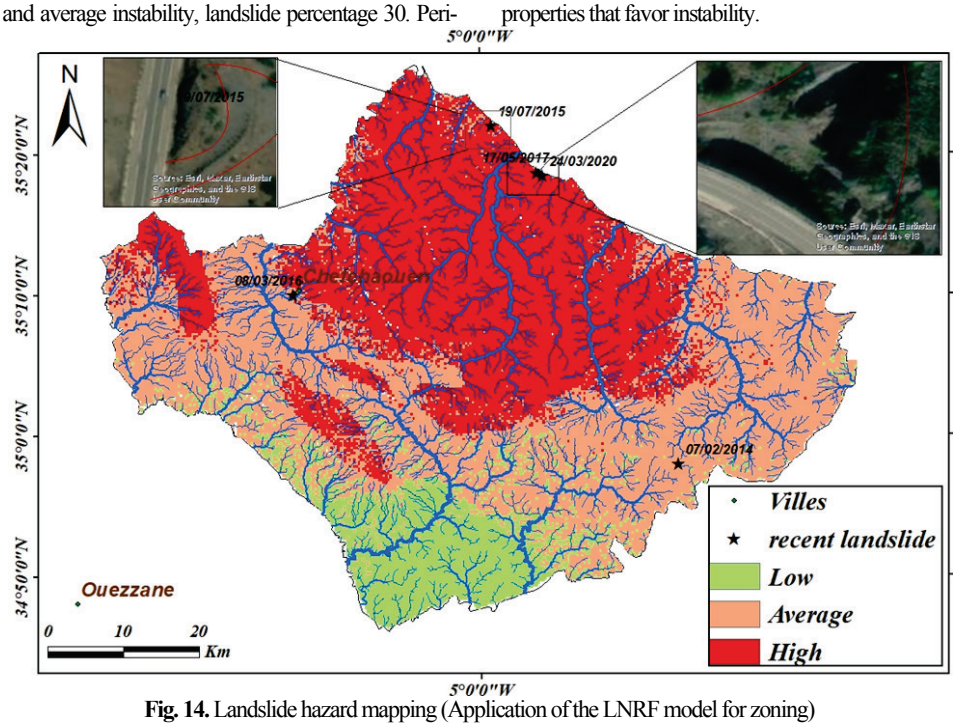

Fig. 14. Landslide hazard mapping (Application of the LNRF model for zoning)

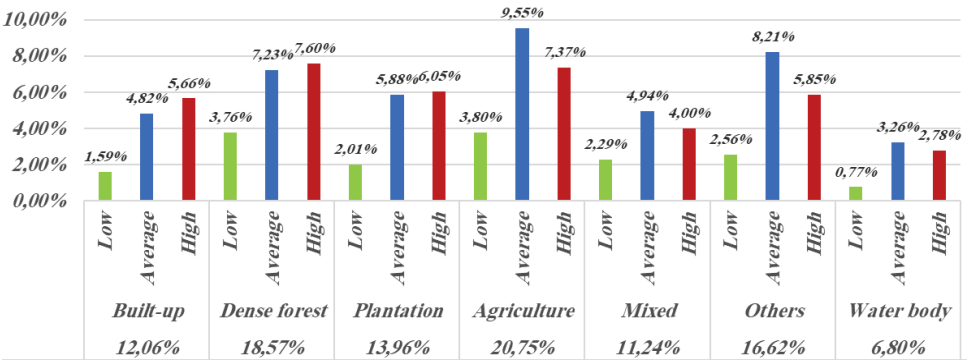

Fig. 15. Distribution of land use types and landslide susceptibility

Lineaments are linear features in the landscape that can reveal underlying geological structures such as faults and joints. They are important for understanding slope stability and landslide occurrence. Proximity to active fault zones, degree of fracturing and junction with the slope are critical factors in determining slope stability. Landslides are more likely to occur in areas with linear patterns or lineaments, and the presence of active faults can increase the risk of landslides. In the study of landslide susceptibility in the Western Ghats of India, lineaments were considered as one of the influencing factors for assessing landslide susceptibility in the study area (Kuriakose et al., 2009; Bhargavi & Arunnehru, 2021; Ajin et al., 2022; Morino et al., 2022; Sadiq et al., 2022).

Precipitation plays a crucial role in slope instability and landslides. In mountainous areas, landslides are often associated with intense precipitation events over a short period, or with prolonged periods of low- to medium-intensity precipitation. Precipitation can saturate the soil, increasing water infiltration and reducing the soil's retention capacity, which in turn can increase the risk of landslides (Stokes et al., 2014; Li et al., 2020; Amarasinghe et al., 2023).

Land Use and Land Cover (LULC) and landslides are interconnected. The land use and land cover (LULC) percentage graph, along with associated landslide susceptibility classes and digital risk factors (LNRF), provides a comprehensive overview (Fig. 14). Among the different land cover classes, buildings occupy 12.1% of the area, exhibiting varying degrees of susceptibility to landslides. Dense forests, representing 18.6% of the total area, show a significant portion with medium to high susceptibility to landslides. Plantations cover 14.0% of the area with a balanced distribution of landslide susceptibility. Agriculture, the largest land cover category at 20.8%, exhibits a considerable percentage with medium to high susceptibility to landslides. Mixed land covers, accounting for 11.2% of the area, mostly show low to medium susceptibility to landslides. Changes in land use, such as deforestation and urbanization, can increase the risk of landslides. LULC mapping, which involves the analysis of satellite images and the use of geographic information systems, plays a key role in understanding these dynamics and putting into action management measures to minimize the risk of landslides (Comber et al., 2004; Pacheco Quevedo et al., 2023; Rong & Fu, 2023). The data provided enables a detailed analysis of land distribution and landslide risk in the study area. Looking at the different land use categories (LULC), plantations and built-up land represent significant proportions of the area, with 14% and 12% respectively. Plantations are particularly prone to landslides, with an affected area of 68%, while built-up areas also record a notable percentage of 30%. Dense forests, farmland and mixed residential and agricultural areas, on the other hand, seem less affected by this phenomenon. Numerical risk factor data confirms this trend, with plantations showing the highest level of risk (4.79), followed by built-up areas (2.12). Fuzzy membership values show a strong correlation between plantations and landslide

risk, with a maximum fuzzy membership of 1, while built-up land has a significant membership of 0.44. These results are consistent with the weights assigned to the different categories, where plantations and built-up land have significant weights of 2. In terms of landslide instability, affected areas in plantations and built-up land are generally considered to have medium instability (Table 2). Other land types, encompassing 16.6% of the land, exhibit medium susceptibility to landslides in a significant portion. Water bodies, occupying the smallest area at 6.80%, generally exhibit low to medium susceptibility to landslides. The data suggest that certain types of land cover, such as dense forest and agriculture, have higher percentages of areas with medium to high susceptibility to landslides compared to others such as water bodies and buildings.

The normalized difference vegetation index (NDVI) has been established to have an effect on landslide susceptibility maps (LSM). In one study, the effect of NDVI was observed on LSMs created using bivariate and multivariate GIS-based statistical models such as frequency ratio (FR), information value (IoV), multiple linear regression (MLR), and logistic regression (LR). The accuracy of each of these models increased when NDVI was considered as a causal factor. Another study used NDVI as a time-varying factor and found that using time-varying NDVI showed superior performance compared to using NDVI from a specific year only (Lahcen et al., 2022; Doan et al., 2023; Niraj et al., 2023).

Chefchaouen's topographical curvature is influenced by the geological and morphological complexity of the region. The town's relief shows marked contrasts between steep rocky reliefs at higher elevations and gentle clay slopes downhill. These topographical variations are the result of differential erosion processes and the movement of clay formations, creating a rugged topography with poor drainage (Kasai & Yamada, 2019). The region is characterized by mountainous relief, varied geological formations, steep slopes, significant vertical drops and rock faces. The region's geomorphology is influenced by its geological structure, active tectonics, Mediterranean and oceanic climate, as well as by the intense erosive dynamics caused by the deep valleys, steep slopes and steep gradients (Mastere et al., 2015).

Chefchaouen features a wide variability of vegetation cover, with dense forests, matorrals or scrubland, agricultural land, bare land, urbanized areas and bodies of water. The region's geomorphology is also influenced by human activity, including urban expansion, deforestation for agriculture and other anthropogenic activities (El Kharim et al., 2021). Chefchaouen is at risk of earthquakes due to its geographical position in a collision zone between the African and Eurasian tectonic plates. This zone is characterized by high seismic activity, with frequent and sometimes devastating earthquakes. Although Chefchaouen has not experienced any major earthquakes recently, it is important to take seismic risk into account in urban planning and building construction. Seismic construction standards must be respected to minimize the risk of damage and loss in the event of an earthquake. It is also important to raise public awareness of seismic risks and to put in place emergency plans to deal with any natural disasters (El Kharim et al., 2021; Wang et al., 2021).

Precipitation can have a significant impact on land instability. High rainfall can saturate the soil, increasing the risk of landslides. In our study, we noted 9 precipitation intervals ranging from 1705 to 1967 mm. When rainfall is between 1734 and 1764 mm, we observe that the landslide zone is 30%. The Numerical Terrain Risk Factor, or LNRF, is 2.72. The fuzzy membership values using the LNRF model are 0.58, with a weight of 2. This indicates average terrain instability. In the rainfall interval between 1880 and 1909 mm, the landslide area is 16%. The LNRF is 1.45. The fuzzy membership values using the LNRF model are 0.31, with a weight of 2. This indicates high terrain instability. Finally, when rainfall is between 1909 and 1938 mm, the landslide area is 52%. The LNRF is 4.7. The fuzzy membership values using the LNRF model are 2, with a weight of 2 (Table 2). This also indicates a high instability of the terrain observations clearly show that precipitation has a direct impact on land instability and the risk of landslides.

To assess the reliability and performance of the GIS-based LNRF technique in estimating landslide-prone areas, the Receiver Operating Characteristic (ROC) method was used. The ROC curve is a useful tool for assessing the quality of a forecasting system, and the area under the curve (AUC) can be used to determine the overall model.

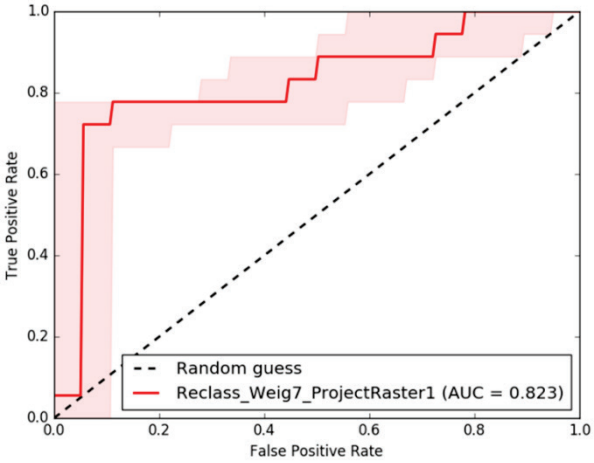

Fig. 16. Performance evaluation of landslide models using ROC curve analysis

In this study, landslide point inventory data from the Geological Survey of India were used as data. The ROC curve was used to assess the overall performance of the landslide models on the test datasets. The success rate was determined by comparing the test data with the landslide susceptibility map (Fig. 16). The LNRF model achieved an AUC value of 0.823, indicating good prediction performance and reliable results for the landslide susceptibility map. These results reveal that the GIS-based LNRF technique is a reliable and effective method for estimating landslide susceptibility areas.

The Numerical Landslide Risk Factor (LNRF) study is a complex area of research. Challenges and limitations associated with the study of landslide risk factors include study scale, data availability and quality, methodology, risk perception by populations and stakeholders, and the use of spatial analysis techniques and GIS technologies. For example, there are no studies on the automatic mapping of landslide risk on a large scale (1:10,000). Furthermore, the availability and quality of data on environmental predisposing factors and the spatial occurrence of past and present landslides can pose a challenge. Depending on the scale of the study and the difficulty of implementing the quantitative analytical approach, the empirical analytical approach is often preferred. Finally, the perception of risk by populations and stakeholders can vary, which can affect the effectiveness of prevention measures, and spatial analysis techniques and GIS technologies are rarely used to assess and map landslide risk. These limitations and challenges can affect the accuracy and applicability of the results of these studies. It is important to take these factors into account when designing their studies and interpreting their results.

Conclusion

The study highlights the complexity of landslide risks in Chefchaouen, influenced by multiple factors including precipitation, topography, geology, and land use. Our analysis demonstrates that heavy precipitation, steep slopes, and high altitudes significantly increase landslide vulnerability. Additionally, specific soil types like clays and land uses such as plantations and urban areas exacerbate these risks. Integrating these factors into risk assessments is crucial for effective management.

An integrated approach is essential for managing landslide risks, involving proactive land management, prevention strategies, and monitoring. The GIS-based LNRF model, validated through ROC analysis, provides reliable estimates of landslide-prone areas, aiding informed decision-making and risk reduction.

To mitigate landslide risks in Chefchaouen, it is vital to implement comprehensive measures, including risk assessments, land use regulations, improved drainage systems, and reforestation. Public awareness, enhanced meteorological and geological monitoring, and coordinated efforts among local authorities will further support effective risk management in this geologically and climatically challenging region.

We would like to acknowledge the support and assistance of the local authorities in Chefchaouen, Morocco, as well as the contributions from the research teams and

institutions that provided valuable data and insights for this study. Special thanks to the remote sensing and GIS specialists whose expertise greatly enhanced the quality of our analysis.

References

Abedini, M., & Tulabi, S. (2018). Assessing LNRF, FR, and AHP models in landslide susceptibility mapping index: A comparative study of Nojian watershed in Lorestan province, Iran. Environmental Earth Sciences, 77(11), 1–13.

Ajin, R. S., Nandakumar, D., Rajaneesh, A., Oommen, T., Ali, Y. P., & Sajinkumar, K. S. (2022). The tale of three landslides in the Western Ghats, India: Lessons to be learnt. Geoenvironmental Disasters, 9(1), 1–8.

Alcántara-Ayala, I., & Sassa, K. (2023). Landslide risk management: From hazard to disaster risk reduction. Landslides, 20(10), 2031–2037.

Amarasinghe, M. P., Kulathilaka, S. A. S., Robert, D. J., Zhou, A., & Jayathissa, H. A. G. (2023). Risk assessment and management of rainfall-induced landslides in tropical regions: A review. Natural Hazards, 120(3), 2179–2231.

Arabameri, A., Pradhan, B., Rezaei, K., Sohrabi, M., & Kalantari, Z. (2019). GIS-based landslide susceptibility mapping using numerical risk factor bivariate model and its ensemble with linear multivariate regression and boosted regression tree algorithms. Journal of Mountain Science, 16(3), 595–618.

Bhargavi, G., & Arunnehru, J. (2021). Land risk susceptibility, hazard and risk factors in Western Ghats, India – A review. International Journal of Environmental Science, 6, 1–10.

Bouchra, A., Mustapha, H., & Mohammed, R. (2020). D-InSAR analysis of Sentinel-1 data for landslide detection in Northern Morocco, case study: Chefchaouen. Journal of Geoscience and Environment Protection, 8(7), 84–103.

Comber, A. J., Law, A. N. R., & Lishman, J. R. (2004). Application of knowledge for automated land cover change monitoring. International Journal of Remote Sensing, 25(16), 3177–3192.

Doan, V. L., Nguyen, B. Q. V., Pham, H. T., Nguyen, C. C., & Nguyen, C. T. (2023). Effect of time-variant NDVI on landside susceptibility: A case study in Quang Ngai province, Vietnam. Open Geosciences, 15(1), 20220550.

Doljin, D., & Yembuu, B. (2021). The relief and geomorphological characteristics of Mongolia. In: Yembuu, B. (Ed.). The physical geography of Mongolia. Springer, Cham. Pp. 23–50.

El Kharim, Y., Bounab, A., Ilias, O., Hilali, F., & Ahniche, M. (2021). Landslides in the urban and suburban perimeter of Chefchaouen (Rif, Northern Morocco): inventory and case study. Natural Hazards, 107(1), 355–373.

Gruzelle, A., & Lebaut, S. (2022). Démarche d'analyse et de diagnostic du risque de glissement de terrain: De l'identification à une mesure proactive. Physio-Geo, 17, 167–192.

Ibrahim, M., Al-Mashaqbah, A., Koch, B., & Datta, P. (2020). An evaluation of available digital elevation models (DEMs) for geomorphological feature analysis. Environmental Earth Sciences, 79, 336.

Kasai, M., & Yamada, T. (2019). Topographic effects on frequency-size distribution of landslides triggered by the Hokkaido Eastern Iburi Earthquake in 2018. Earth, Planets and Space, 71(1), 89.

Kuriakose, S. L., Sankar, G., & Muraleedharan, C. (2009). History of landslide susceptibility and a chorology of landslide-prone areas in the Western Ghats of Kerala, India. Environmental Geology, 57(7), 1553–1568.

Lahcen, D., Hafida, N., Souad, M., Rachid, E. H., Bejjaji, Z., & Mohamed, S. (2022). Integration of remote sensing and GIS in the identification of the vegetation covers degradation of the korifla basin (NW of Central Morocco) between 1990 and 2018. IOP Conference Series: Earth and Environmental Science, 975(1), 012001.

Li, Z., Zhang, X., Zhu, R., Zhang, Z., & Weng, Z. (2020). Integrating data-to-data correlation into inverse distance weighting. Computational Geosciences, 24(1), 203–216.

Lissak, C., Bartsch, A., De Michele, M., Gomez, C., Maquaire, O., Raucoules, D., & Roulland, T. (2020). Remote sensing for assessing landslides and associated hazards. Surveys in Geophysics, 41(6), 1391–1435.

Margreth, A. (2017). Origins of low-relief plateaus. Nature Geoscience, 10(8), 541–542.

Marín-Rodríguez, N. J., Vega, J., Zanabria, O. B., González-Ruiz, J. D., & Botero, S. (2024). Towards an understanding of landslide risk assessment and its economic losses: A scientometric analysis. Landslides, 21, 1865–1881.

Mastere, M., Van Vliet-Lanoë, B., & Brahim, L. A. (2013). Cartographie de l'occupation des sols en relation avec les mouvements gravitaires et le ravinement dans le Rif nord-occidental (Maroc). Geomorphologie, 19(3), 335–352.

Mastere, M., Van-Vliet Lanoë, B., Ait Brahim, L., & El Moulat, M. (2015). A linear indexing approach to mass movements susceptibility mapping. Revue Internationale de Géomatique, 25(2), 245–265.

Method, L., & Bahnassy, M. H. (2023). Evaluation of landslide risk with the landslide numerical risk factor. Journal of Geology and Geophysics, 12(6), 1114.

Morino, C., Coratza, P., & Soldati, M. (2022). Landslides, a key landform in the global geological heritage. Frontiers in Earth Science, 10, 864760.

Nakileza, B. R., & Nedala, S. (2020). Topographic influence on landslides characteristics and implication for risk management in upper Manafwa catchment, Mt Elgon Uganda. Geoenvironmental Disasters, 7(1), 27.

Niraj, K. C., Singh, A., & Shukla, D. P. (2023). Effect of the normalized difference vegetation index (NDVI) on GIS-enabled bivariate and multivariate statistical models for landslide susceptibility mapping. Journal of the Indian Society of Remote Sensing, 51(8), 1739–1756.

Obda, O., El Kharim, Y., Obda, I., Ahniche, M., & Sahrane, R. (2024a). Landslide susceptibility assessment and factors' selection using the GIS matrix method (GMM) in Chefchaouen Province (Northern Morocco). In: Çiner, A. et al. (Eds.). Recent research on geotechnical engineering, remote sensing, geophysics and earthquake seismology. Springer, Cham. Pp. 197–199.

Ouahabi, M. E., Daoudi, L., & Fagel, N. (2018). Technological behaviour of Cretaceous and Pliocene clays of Northern Morocco used in fired brick manufacturing. Journal of Materials and Environmental Sciences, 9(4), 1140–1151.

Pacheco Quevedo, R., Velastegui-Montoya, A., Montalván-Burbano, N., Morante-Carballo, F., Korup, O., & Daleles Rennó, C. (2023). Land use and land cover as a conditioning factor in landslide susceptibility: A literature review. Landslides, 20(5), 967–982.

Pande, C. B., Srivastava, A., Moharir, K. N., Radwan, N., Mohd Sidek, L., Alshehri, F., Pal, S. C., Tolche, A. D., & Zhran, M. (2024). Characterizing land use/land cover change dynamics by an enhanced random forest machine learning model: A google earth engine implementation. Environmental Sciences Europe, 36(1), 84.

Papathoma-Köhle, M., Neuhäuser, B., Ratzinger, K., Wenzel, H., & Dominey-Howes, D. (2007). Elements at risk as a framework for assessing the vulnerability of communities to landslides. Natural Hazards and Earth System Science, 7(6), 765–779.

Patil, A. S., & Panhalkar, S. S. (2023). Remote sensing and GIS-based landslide susceptibility mapping using LNRF method in part of Western Ghats of India. Quaternary Science Advances, 11, 100095.

Patil, A. S., Bhadra, B. K., Panhalkar, S. S., & Patil, P. T. (2020). Landslide susceptibility mapping using landslide numerical risk factor model and landslide inventory prepared through OBIA in Chenab Valley, Jammu and Kashmir (India). Journal of the Indian Society of Remote Sensing, 48(3), 431–449.

Rong, C., & Fu, W. (2023). A comprehensive review of land use and land cover change based on knowledge graph and bibliometric analyses. Land, 12(8), 1573.

Rovero, L., & Fratini, F. (2013). The Medina of Chefchaouen (Morocco): A survey on morphological and mechanical features of the masonries. Construction and Building Materials, 47, 465–479.

Roy, J., & Saha, S. (2019). Landslide susceptibility mapping using knowledge driven statistical models in Darjeeling District, West Bengal, India. Geoenvironmental Disasters, 6(1), 11.

Sadiq, S., Muhammad, U., & Fuchs, M. (2022). Investigation of landslides with natural lineaments derived from integrated manual and automatic techniques applied on geospatial data. Natural Hazards, 110(3), 2141–2162.

Şen, Z., & Şişman, E. (2024). Probabilistic standardization index adjustment for standardized precipitation index (SPI). Theoretical and Applied Climatology, 155(4), 2747–2756.

Stokes, A., Douglas, G. B., Fourcaud, T., Giadrossich, F., Gillies, C., Hubble, T., Kim, J. H., Loades, K. W., Mao, Z., McIvor, I. R., Mickovski, S. B., Mitchell, S., Osman, N., Phillips, C., Poesen, J., Polster, D., Preti, F., Raymond, P., Rey, F., … Walker, L. R. (2014). Ecological mitigation of hillslope instability: Ten key issues facing researchers and practitioners. Plant and Soil, 377, 1–23.

Sur, U., Singh, P., Rai, P. K., & Thakur, J. K. (2021). Landslide probability mapping by considering fuzzy numerical risk factor (FNRF) and landscape change for road corridor of Uttarakhand, India. Environment, Development and Sustainability, 23(9), 13526–13554.

Taalab, K., Cheng, T., & Zhang, Y. (2018). Mapping landslide susceptibility and types using random forest. Big Earth Data, 2(2), 159–178.

Tyagi, A., Tiwari, R. K., & James, N. (2023). Mapping the landslide susceptibility considering future land-use land-cover scenario. Landslides, 20(1), 65–76.

Wang, W., Wang, J., & Romanowicz, R. (2021). Uncertainty in spi calculation and its impact on drought assessment in different climate regions over China. Journal of Hydrometeorology, 22(6), 1369–1383.

Yang, Z., Lu, H., Zhang, Z., Liu, C., Nie, R., Zhang, W., Fan, G., Chen, C., Ma, L., Dai, X., Zhang, M., & Zhang, D. (2023). Visualization analysis of rainfall-induced landslides hazards based on remote sensing and geographic information system – an overview. International Journal of Digital Earth, 16(1), 2374–2402.

Yong, C., Jinlong, D., Fei, G., Bin, T., Tao, Z., Hao, F., Li, W., & Qinghua, Z. (2022). Review of landslide susceptibility assessment based on knowledge mapping. Stochastic Environmental Research and Risk Assessment, 36(9), 2399–2417.